Journal of Power Sources 187 (2009) 90–92

Contents lists available at ScienceDirect

Journal of Power Sources

journal homepage: www.elsevier.com/locate/jpowsour

Short communication

Fabrication and characterization of an anode-supported hollow fiber SOFC

Chunli Yang, Wei Li, Shangquan Zhang, Lei Bi, Ranran Peng, Chusheng Chen, Wei Liu*

Laboratory of Advanced Functional Materials and Devices, Department of Materials Science and Engineering, University of Science and Technology of China, Hefei, Anhui 230026 PR China

ARTICLE INFO

Article history:
Received 18 September 2008
Received in revised form 18 October 2008
Accepted 20 October 2008
Available online 28 October 2008

Keywords:
Solid oxide fuel cells
Ni-YSZ anode-supported
Hollow-fiber
Phase inversion

ABSTRACT

In this study, an anode-supported hollow-fiber solid oxide fuel cell (SOFC) of diameter 1.7 mm has been successfully fabricated using the phase inversion and vacuum assisted coating techniques. The cell has a special structure consisting of a 12-μm-thick yttria-stabilized zirconia (YSZ) electrolyte film and a Ni-YSZ anode layer which has large finger-like pores on both sides of the hollow-fiber membrane. The hollow-fiber SOFC has an active electrode area of 0.63 cm^2 and generates maximum power densities of 124, 287 and 377 mW cm^{-2} at 600, 700 and 800 °C, respectively, indicating that its use in applications requiring high power density is promising.

1. Introduction

In recent years, solid oxide fuel cells (SOFCs) have received considerable attention as a keystone of the future energy economy due to their many distinct advantages such as extremely high efficiencies, low pollution and fuel flexibility [1–5]. Amongst SOFCs, the state-of-the-art electrolyte is the yttria-stabilized zirconia (YSZ) ceramic, which exhibits good thermal and chemical stability, high oxygen ion transfer number, and great mechanical strength at high temperature. The most frequently used anode materials are Ni-YSZ composites, which display excellent catalytic properties for fuel oxidation and good current collection. The other key component in the SOFCs is the cathode, and Sr-doped lanthanum manganate ($La_{0.8}Sr_{0.2}MnO_3$) is most commonly used for this because it is an effective catalyst for the dissociation of oxygen molecules and has high electronic conductivity in a highly oxidizing environment [2,4,6–8].

Nowadays, planar and tubular geometric configurations are the main SOFC designs. The tubular type is relatively mature in terms of designing and manufacturing technology and has attracted much interest because it has better thermo-cycling behavior and is easier to seal, compared with the planar design [3,9–11]. Moreover, it is interesting to note that several potential benefits appear when the diameter gets smaller, on the micron scale. The micro-tubular designs can achieve higher volumetric power density because this scales with the reciprocal of the tube diameter. They also possess high thermal shock resistance, which is a distinct advantage in applications where start-up time is critical [11,12].

The substrate of the micro-tubular SOFCs is often fabricated by traditional extrusion techniques [1,13–15]. The as-prepared tubes usually have a poor microstructure which gives rise to a larger resistance. Recently, ceramic hollow-fiber membranes with an asymmetric structure prepared by an immersion induced phase inversion method have been employed to fabricate tubular SOFCs [16]. The YSZ hollow-fiber SOFC offers a high and stable open voltage (near 1.2 V), and its maximum power density is about 18 mW cm^{-2} at 800 °C. However, the power density of this type of electrolyte-supported SOFC is relatively low, because of the high electrolyte ohmic loss. Therefore, an effective approach to achieve high performance should be the minimization of the thickness of the electrolyte layer, a design similar to anode-supported cells. In this work, anode-supported hollow-fiber SOFCs with diameters less than 2 mm were fabricated by the phase inversion and vacuum assisted coating techniques with a co-firing process. Electrochemical evaluation of the unit cell was performed and analyzed by study of their *V–I* characteristics and impedance spectra in the temperature range 600–800 °C.

2. Experimental

8YSZ (FUCIDE, Anhui, China) and NiO powders with a weight ratio of 40:60 were used as the anode materials. *N*-methyl-2-pyrrolidone (NMP, CP, SCRC, China), polyethersulfone (PESf, Radel A-100, Solvay Advanced Polymers, L.L.C.) and polyvinylpyrrolidone

* Corresponding author. Tel.: +86 551 3606929; fax: +86 551 3602586.
E-mail address: wliu@ustc.edu.cn (W. Liu).

0378-7753/$ – see front matter © 2008 Elsevier B.V. All rights reserved.
doi:10.1016/j.jpowsour.2008.10.069

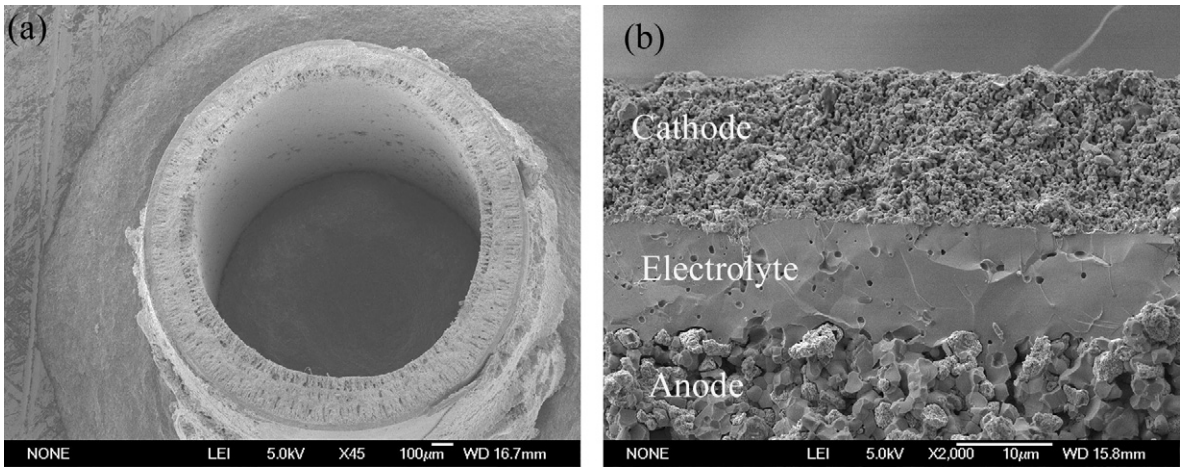

Fig. 1. Cross-sectional SEM images of the anode-supported hollow-fiber cell after testing: (a) overall view and (b) enlarged view.

(PVP, K30, CP, SCRC, China) were used as the solvent, binder and dispersant, respectively. The ceramic powders were dispersed uniformly in the polymer solution using a planetary ball mill for 2 days at the speed of 100 r min^{-1}.The duration was influenced both by the viscosity of the solution and the rotation speed of planetary milling. A tube-in-orifice spinneret with out diameter/inner diameter of 2.6/1.0 mm was used to obtain the anode hollow fiber precursors. Tap water was used as both the internal and external coagulants for all spinning runs. The hollow-fiber precursors were then immersed in water for 1 day to ensure complete solidification and pre-sintered at 1200 °C for 5 h.

A YSZ electrolyte layer was coated on to the surface of the pre-sintered hollow-fiber membrane using a vacuum assisted coating technique and then co-fired at 1450 °C for 10 h to form a thin and dense layer. The cathode materials $(La_{0.8}Sr_{0.2})_{0.95}MnO_3$ (LSM) and 8YSZ (1:1 wt%) were coated on to the electrolyte by brush printing and sintered at 1150 °C for 3 h. The dimensions of the hollow-fiber cell were 0.17 cm in diameter and 10 cm in length with the cathode length 1.18 cm and the active electrode area 0.63 cm^2. The Voltage–current (*V–I*) characteristics of the cell were investigated with a dc Electronic Load tester (IT8511) and the ac impedance under open-circuit conditions was investigated using a CHI604C (0.1 Hz to 100 KHz) in the temperature range 600–800 °C. The fiber was connected on both sides with small-diameter alumina tubes and sealed with Ag paste. The outer shell of the fiber was exposed to the ambient air, and the core side was swept with wet H_2 (~3% H_2O) with a flow rate of about 40 ml min^{-1}. The current collection from the electrodes was conducted by winding Ag wires around the cathode and along the edge of the anode hollow-fiber, where the both Ag wires were fixed using Ag paste. The experimental apparatus was similar to that of Ref. [1]. A scanning electron microscope (SEM, JSM-6301F) was used to check the microstructure of the cell after testing.

3. Results and discussion

Fig. 1 presents cross-sectional SEM images of the anode-supported hollow-fiber cell after testing. As seen in Fig. 1(a), the thickness of the anode membrane is about 150 μm. A finger-like porous structure is formed near both surfaces of the hollow-fiber which provides a convenient channel for transporting the fuel gas to the electrolyte. A 12-μm-thick YSZ electrolyte membrane was successfully coated on the anode hollow-fiber by vacuum assisted coating and co-sintering method, as shown in Fig. 1(b). The electrolyte is extremely dense, without any cracks, and adheres very well to both the Ni-YSZ anode and the LSM-YSZ cathode layers.

The electrochemical performance of the Ni-YSZ anode-supported hollow-fiber cell at various temperatures is presented in Fig. 2. The open-circuit voltage (OCV) varies from 1.01 to 1.03 V with temperature, which is close to the theoretical value predicted by the Nernst equation for each temperature. The high OCV means that the gas leakage through the electrolyte is negligible and the prepared electrolyte is a dense layer without any cracks and defects.

The maximum power densities of 124, 287, and 377 mW cm^{-2} are achieved at 600, 700 and 800 °C, respectively, which are dozens of times higher than that of the electrolyte-supported cell [16]. The higher peak power densities are probably due to the use of the much thinner electrolyte membrane, which reduces the ohmic polarization from the electrolyte during the cell operation. In addition, the maximum power densities are also superior to those of the planar cell with a 14.9 μm YSZ electrolyte film fabricated by a spray coating technique below 700 °C [7], which may be due to the large finger-like pores in the anode layer.

I–V plots are slightly curved at the measured temperatures, especially at low temperature, which implies insufficient electrochemical activity at the cathode side [13]. Therefore, the cell performances may be further improved by using graded electrodes and optimizing the electrode microstructure to decrease the electrode polarization. To explore the polarization phenomena of the

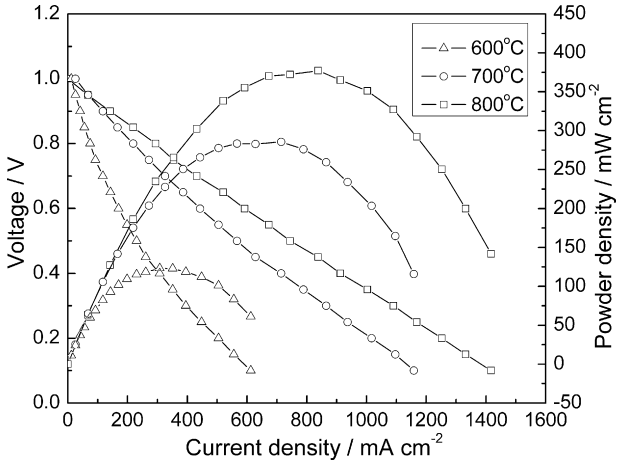

Fig. 2. Voltage–current (*V–I*) characteristics of the Ni-8YSZ anode-supported hollow-fiber cell at various temperatures.

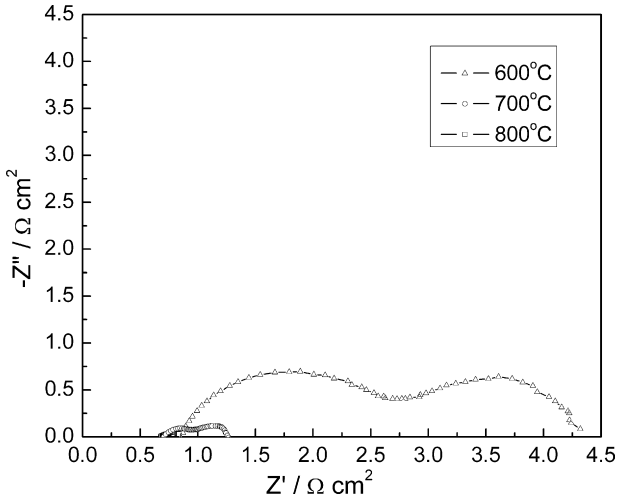

Fig. 3. ac impedance spectra of the hollow-fiber cell under open-circuit conditions at various temperatures.

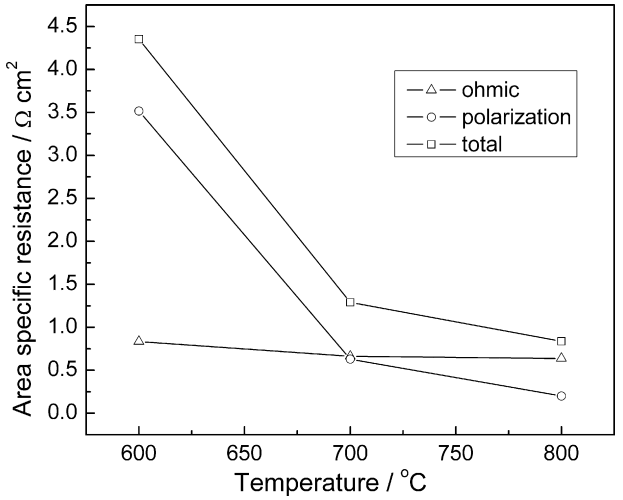

Fig. 4. Area specific values of the ohmic, polarization and total resistances of the hollow-fiber cell under open-circuit conditions at various temperatures.

fabricated unit cell, impedance spectra were measured under open-circuit conditions and these are shown in Fig. 3. The low frequency intercept corresponds to the total resistance, including ohmic resistance, activation polarization resistance, and concentration polarization resistance. The high frequency intercept represents the ohmic resistance of the cell, involving ionic resistance of the electrolyte and electronic resistance of the electrodes [17]. The ohmic, polarization and total resistances obtained from the impedance spectra are summarized in Fig. 4. It can be seen that the interfacial polarization resistance is large at low temperature, whereas the ohmic resistance becomes dominant at high temperature, where the cell performance mainly depends on the ohmic resistance. In addition, the ohmic resistance decreases only slightly with decreasing temperature, which can be attributed to the extra anodic resistance because of the current collection method [1,13,18]. Current collection from the anode was only made from one edge of the anode hollow-fiber. The long current path generates high ohmic resistance along with the hollow-fiber, including ohmic and electrode overpotential resistance [18]. For further improvement of hollow-fiber cell performance, therefore, the current collecting problem at the anode side needs to be solved. This is currently under investigation.

4. Conclusions

An anode-supported hollow-fiber SOFC of diameter 1.7 mm has been successfully fabricated using the phase inversion and vacuum assisted coating techniques and evaluated over the temperature range 600–800 °C. The cell has a special structure with a 12-μm-thick dense YSZ electrolyte film and a Ni-YSZ anode layer with large finger-like pores on both sides of the hollow-fiber membrane. The OCV values are greater than 1.01 V and the maximum power densities reach 124, 287, and 377 mW cm^{-2} at 600, 700 and 800 °C, respectively, using wet H_2 (~3% H_2O) as fuel and static air as oxidant gas. As a result of high packing densities, this kind of anode-supported hollow-fiber SOFCs has a high potential for practical applications.

Acknowledgements

The research was supported by the Key Program of Chinese Academy of Science (no. KJCX1. YWo7) and National High-tech R&D Program of China (no. 2007AA05Z157).

References

[1] T. Suzuki, T. Yamaguchi, Y. Fujishiro, M. Awano, J. Power Sources 160 (2006) 73–77.
[2] A. Atkinson, S. Barnett, R.J. Gorte, J.T.S. Irvine, A.J. Mcevoy, M. Mogensen, Nat. Mater. 3 (2004) 17–27.
[3] N.M. Sammes, Y. Du, R. Bove, J. Power Sources 145 (2005) 428–434.
[4] R.J. Gorte, S. Park, J.M. Vohs, C. Wang, Adv. Mater. 12 (2000) 1465–1469.
[5] S.W. Tao, J.T.S. Irvine, J.A. Kilner, Adv. Mater. 17 (2005) 1734–1737.
[6] S. Tao, J.T.S. Irvine, Nat. Mater. 2 (2003) 320–323.
[7] J. Ding, J. Liu, Solid State Ionics 179 (2008) 1246–1249.
[8] B.A. Boukamp, Nat. Mater. 2 (2003) 294–296.
[9] Y. Liu, S.I. Hashimoto, H. Nishino, K. Takei, M. Mori, T. Suzuki, Y. Funahashi, J. Power Sources 174 (2007) 95–102.
[10] A.V. Akkaya, Int. J. Energy Res. 31 (2007) 79–98.
[11] J. Jia, R. Jiang, S. Shen, A. Abudula, Environ. Energy Eng. 54 (2008) 554–564.
[12] S.C. Singhal, K. Kendall, High Temperature Solid Oxide Fuel Cells: Fundamentals, Design and Applications, Elsevier, New York, 2003, pp. 219.
[13] T. Yamaguchi, S. Shimizu, T. Suzuki, Y. Fujishiro, M. Awano, Mater. Lett. 62 (2008) 1518–1520.
[14] Y. Funahashi, T. Shimamori, T. Suzuki, Y. Fujishiro, M. Awano, J. Power Sources 163 (2007) 731–736.
[15] T. Suzuki, Y. Funahashi, T. Yamaguchi, Y. Fujishiro, M. Awano, J. Alloys Compd. 451 (2008) 632–635.
[16] C.C. Wei, K. Li, Ind. Eng. Chem. Res. 47 (2008) 1506–1512.
[17] C. Xia, M. Liu, Adv. Mater. 14 (2002) 521–523.
[18] T. Suzuki, Y. Funahashi, T. Yamaguchi, Y. Fujishiro, M. Awano, J. Power Sources 171 (2007) 92–95.